Adaptive and Reference Shaping Control for Steer-By-Wire Vehicles in High-Speed Maneuvers

Srivatsan Srinivasan, Matthias J.Schmid, Venkat Krovi

Dept. of Automotive Eng., Clemson University, Greenville, SC 29607
(e-mails: srivats@clemson.edu, schmidm@clemson.edu, vkrovi@clemson.edu).

Abstract: The growing adoption of steer-by-wire (SbW) systems in (semi-)autonomous vehicles provide a unique opportunity to exploit steering control for vehicle stability systems. In our previous work, we introduced a feedforward controller for an SbW vehicle employing optimal reference shaping and demonstrated reduced yaw disturbances during fast (evasive) maneuvers. Despite its beneficial effect on damping undesirable oscillations, open-loop input shaping can lead to unreliable trajectory tracking without additional feedback compensation in the presence of parameter inaccuracies and model uncertainties. In this study, we significantly advance the previous idea by combining a model reference adaptive control (MRAC) framework with an input shaper. Here, the MRAC framework converges quickly and maintains a nominal 'inner loop' behavior for the input shaper during high-speed maneuvers. This work includes stability and boundedness proof as well as extensive simulations.

Keywords: Vehicle dynamic systems, Adaptive control of automotive systems, Steer-by-wire control, Automotive control, Reference shaping control

1. INTRODUCTION

The rise of Advanced Driver Assistance Systems (ADAS) and autonomous vehicles has led to new avenues for the development of technologies focusing on road safety. The responsibility of ensuring stability during sudden maneuvers, unexpected disturbances, sensor failure, loss of function, etc. no longer rests solely on the driver (Campbell et al., 2010). Recently, there has been a significant shift from active safety sub-systems (e.g. Electronic Stability Control (ESC)) to ADAS systems (e.g. Lane Keep Assist) (Kalra, 2017). Active steering control now has the potential to augment/complement the traditional differential braking or torque distribution systems.

In sudden steering situations performed at high speed, disturbance attenuation (yaw control) whilst following a prescribed trajectory is not easily manageable (Rajamani, 2012). The main objective of a (supportive) steering controller is to compensate for inadequate reference inputs, arising either from a human driver or an ADAS planner. Additionally, it also provides an opportunity to compensate for unexpected dynamics without compromising on path/trajectory tracking. Steer-by-Wire (SbW) systems could be a suitable addition for yaw stability control during high-speed emergency maneuvers. When no physical steering column is present, preventative strategies rather than mitigative strategies (e.g. ESC) could be deployed by timely intervention. The opportunity to be proactive instead of reactive allows for rethinking some of the pre-existing active safety systems. The adoption of SbW as a technology has already found its way into the mainstream automotive industry (Arango et al., 2020).

In our previous work, Srinivasan et al. (2019), we demonstrated the merit of extending steering control as a means for yaw stabilization by introducing a feedforward SbW controller based on the concept of optimal reference shaping. This pre-filtering technique is computationally inexpensive and can act as a fail-safe during total sensor loss. Despite its promising effect on undesirable transients, the previously introduced stand-alone configuration proved itself unreliable for trajectory tracking without additional feedback compensation, as it was highly dependent on modeling accuracy and parameter knowledge. Systems with parameter uncertainty and complex nonlinear dynamics in some areas of the operating domain are prime applications for adaptive control methods that can effectively cope with some parameter as well as modeling errors (Slotine and Li, 2005; Kalur et al., 2016).

Several studies have employed a Model Reference Adaptive Control (MRAC) scheme for steering control in vehicles for path following or yaw stability (Fukao et al., 2001; Ahmadian et al., 2021; Byrne and Abdallah, 1995; Mitov et al., 2020; Vempaty et al., 2016). A combination of reference shaping and adaptive control techniques has also been explored for flexible structures and robot manipulators by effectively enforcing linear behavior (Tzes and Yurkovich, 1993; Khorrami et al., 1993). While robotic manipulators usually operate at slower speeds (thus being very suited for adaptive control), vehicles might require operation at the limit where safety is of great concern.

In this study, we advance the previous feedforward control idea by combining the reference shaping controller with an MRAC framework to reasonably maintain nominal lin-

ear behavior for the input shaper even during high-speed maneuvers. The remainder of the paper is organized as follows: section 2 briefly summarizes our previous work and sets up the problem for our study. Section 3 presents the background and design approach of the employed adaptive control scheme. Here, we also present a Lyapunov-based stability proof for the configuration. Finally, numerical simulation in section 4 is performed to validate the targeted performance before section 5 concludes the study.

Table 1. Parameters in the vehicle model

Symbol	Description	Unit
l_f	Front axle to CG distance	m
l_r	CG to rear axle distance	m
m	Vehicle mass	Kg
I_z	Inertia with respect to z-axis	Kgm^2
g	Gravitational acceleration	m/s^2
$C_{\alpha f,r}$	Front/Rear cornering stiffnesses	Kg/rad
δ	Road-Wheel steering angle	rad
v_x	Longitudinal velocity	m/s
$\dot{y}$	Lateral velocity	m/s
$\dot{\psi}$	Yaw rate	rad/s

2. PRELIMINARY CONSIDERATIONS

In this section we briefly summarize our previous work in Srinivasan et al. (2019) to ensure continuity and context. The general approach utilizes a simplified linear vehicle dynamics model for controller development while numerical evaluation is performed with a high fidelity model as the 'true' plant. Here, a five degrees of freedom (5-DoF) model is utilized. Additionally, the ground-tire interactions consider the wheels as rotating masses (1-DoF) with drive/brake torques while the contact forces are given by the Pacejka tire model (Pacejka, 2009) in combination with a first order slip angle relaxation approach (1-DoF). This yields a model with a total of 18 states. The relevant equations together with a detailed description and nomenclature are provided in Srinivasan et al. (2019). The terms utilized in the vehicle model are summarized in Table 1.

2.1 2-DoF Linear Vehicle Model

For the standard simplified model (Rajamani, 2012), the left and right wheels on each axle are lumped together. Constant longitudinal velocity ($v_x = const$) and small steering angles are assumed with a center of gravity on the ground such that roll and pitch can be neglected. Hence, the model yields 2 degrees of freedom, i.e. one translational (lateral) and one rotational (yaw) motion. This highly simplified linear formulation serves a dual purpose by being employed as the control model for the input shaper and as the reference model for the adaptive control scheme:

$$\dot{\boldsymbol{x}}(t) = A_r \boldsymbol{x}(t) + \boldsymbol{b}_r u(t)$$

$$A_r = \begin{bmatrix} -\dfrac{2C_{\alpha f} + 2C_{\alpha r}}{m v_x} & -v_x - \dfrac{2C_{\alpha f} l_f - 2C_{\alpha r} l_r}{m v_x} \\ -\dfrac{2C_{\alpha f} l_f - 2C_{\alpha r} l_r}{I_z v_x} & -\dfrac{2C_{\alpha f} l_f^2 + 2C_{\alpha r} l_r^2}{I_z v_x} \end{bmatrix}$$

$$\boldsymbol{b}_r = \begin{bmatrix} \dfrac{2C_{\alpha f}}{m} \\ \dfrac{2 l_f C_{\alpha f}}{I_z} \end{bmatrix}, \qquad \boldsymbol{x} = \begin{bmatrix} \dot{y} \\ \dot{\psi} \end{bmatrix}, \qquad u = [\delta] \tag{1}$$

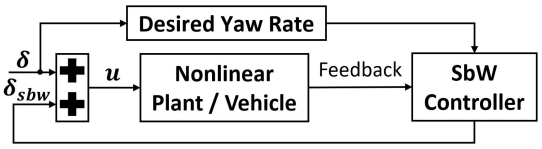

Fig. 1. Control scheme for the standard feedback controller

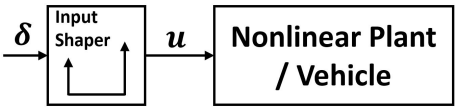

Fig. 2. Control scheme for the feedforward controller

where $\mathbf{x}(t)$ and $u(t)$ are the state and control input vectors, A_r and $\boldsymbol{b}_r$ are the vehicle system and input matrices, and the subscript 'r' refers to the use of Eq. (1) as the reference model in MRAC. As the above system represents the instantaneous linearization at the current operating point, it is a Linear Parameter Varying (LPV) system with C_α rapidly changing during certain maneuvers while v_x mildly varying even when velocity control is enforced. As the reference model in this study, we consider a Linear Time-Invariant (LTI) version, however, nominal parameters are chosen and assumed constant under maneuvering. Nominal cornering stiffnesses are derived from the known tire model of our plant. For small angle approximations, these result as (see Pacejka (2009))

$$C_{\alpha,f/r} = B_{y,f/r}\, C_{y,f/r}\, D_{y,f/r}$$

where B is the stiffness factor, C represents the shape factor, and D denotes the peak factor. These are known parameters for an identified tire, thus providing a reasonable assumption for the nominal value of C_α. Note that the cornering will vary very largely, however, under load transfer or changes in the vehicle.

2.2 Standard Steer-by-wire Feedback Controller

For comparison of our control design, we utilize a standard feedback steering control for yaw stability as given in Rajamani (2012) and as depicted in Fig. 1. Here, the effective steering angle applied to the front wheels consists of the combination of the reference driver (or planner) input with a compensation term generated by the feedback controller to enforce stability and safe maneuvering. The feedback term should only improve stability and safety by reducing the yaw rate error between the actual and (driver) desired yaw rate. It must not interfere with the vehicle's ability to follow the desired path as set by the driver.

2.3 Reference Shaping Control Design

The purpose of an optimal reference shaping controller lies within the prevention and/or fast damping of self-induced transient disturbances, e.g. oscillations in linear or quasi-linear dynamic systems. A vehicle can exhibit excessive oscillatory transients during high-speed maneuvers such as lane change, double lane change, and fishhook (Fancher et al., 1976). This swaying motion might be exacerbated by unnecessary or rather uncoordinated inputs from an untrained driver or a kinematic planner. Reference or input shaping control dampens these effects by placing timely

impulses to attenuate undesired transients. Such a feedforward or pre-filtering technique is advantageous in terms of computational cost, design complexity, and hardware requirements, as it is only based on the convolution of the driver inputs with a series of designed impulses.

Given a system's approximate natural frequency ω_n and damping ratio ζ, the transients caused by a sequence of impulses can be calculated as

$$V(\omega_n,\zeta) = e^{-\zeta\omega_n t_i}\sqrt{E(\omega_n,\zeta)^2 + F(\omega_n,\zeta)^2}$$

$$\text{where} \quad E(\omega_n,\zeta) = \sum_{i=1}^{m} \alpha_i e^{-\zeta\omega_n t_i}\cos(\omega_d t_i)$$

$$\text{and} \quad F(\omega_n,\zeta) = \sum_{i=1}^{m} \alpha_i e^{-\zeta\omega_n t_i}\sin(\omega_d t_i) \tag{2}$$

Here, α_i and t_i are the amplitudes and execution times for the impulse series whereas m is the chosen total number of impulses. As usual, $\omega_d = \omega\sqrt{1-\zeta^2}$ corresponds to the damped natural frequency of the system. As we want to reduce the oscillations caused by the input, we set Eq. (2) equal to 0, and solve for the unknown amplitude and timing, i.e.

$$\begin{bmatrix}\alpha_i \\ t_i\end{bmatrix} = \begin{bmatrix}\frac{1}{1+K} & \frac{K}{1+K} \\ 0 & 0.5\ T_d\end{bmatrix} \tag{3}$$

with $K = \exp(\frac{-\zeta\pi}{1-\zeta^2})$ and T_d being the damped period of the induced transient. In its most basic form, the input shaper can be realized as a 2 impulse filter and hence $i = 1, 2$. For the detailed design process, derivation, and theoretical background, we refer to Srinivasan et al. (2019) and Singh (2019). Figure 2 depicts the simple feedforward architecture.

The same results from our previous study demonstrating the application of this control scheme to a double lane change maneuver (DLC) at 80 km/h are shown in Fig. 3. Note that the chosen maneuver is extremely aggressive given the selected longitudinal velocity. Figure 3 also compares the performance of the input shaper with the standard feedback controller as described in section 2.2. As evident, the best performance is achieved by the combination of the input shaper with the feedback control loop adding only minor computational load. It is important to note that the input shaper will not modulate the raw input signal if it does not cause dynamic instabilities by itself, as illustrated in plots presented in Srinivasan (2021). As a stand-alone controller, however, the reference shaping controller is inferior to the standard feedback regulator. In our previous work, we attributed this behavior to the parametric uncertainty in the control model (2-DoF linearized vehicle) and to the significant modeling errors in comparison to the high fidelity nonlinear plant that is even more pronounced when operating at the dynamic envelope. The sensitivity of input shapers with respect to modeling errors and nonlinearities has long been known and motivated the study of an additional adaptive control loop as introduced in section 3.

3. MODEL REFERENCE ADAPTIVE CONTROL

Reference shaping control utilizing a highly simplified model does not perform adequately as a stand-alone solution for vehicle stability during extreme maneuvers. On the other hand, the standard feedback compensator as described in section 2.2 is still just a proportional controller that experiences known deterioration and robustness issues under disturbances (even when well-tuned). Additionally, nonlinear state and parameter observers/estimators are necessary for proper functionality. Some solutions addressing system uncertainty by utilizing methods such as disturbance observers (Yamaguchi and Murakami, 2009) and GPS-INS-based side-slip estimation for feedforward compensation (Yih and Gerdes, 2005) have been explored successfully, but those techniques are complex and often less than ideal for practical applications. Identifying control parameters accurately online to ensure robust steering performance is still an ongoing challenge.

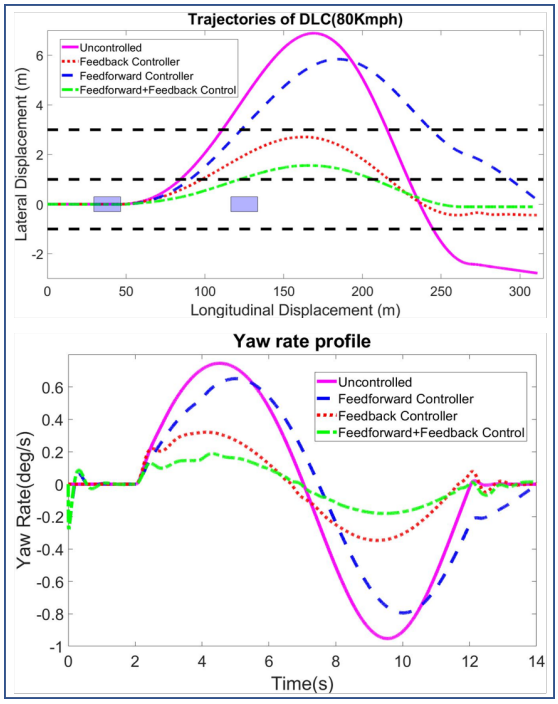

Fig. 3. Plant response plots from previous work

In an alternative approach, we deploy an SbW controller with a direct MRAC scheme to ensure a predictable and fixed relation between a steering command (generated by the driver or planner) and the vehicle output (yaw rate and lateral velocity). The required feedback signals are commonly measured/estimated quantities using inexpensive Inertial Measurement Units (IMUs) that can be found in most vehicles nowadays. In this setting, the primary objective of MRAC is not to achieve an end-to-end control performance, but to adapt for and to stably maintain a nominal input-output behavior. This ideal behavior corresponds to the one prescribed by the bicycle model in Eq. (1). The inner adaptive control loop formed by the MRAC scheme now enforces an input-output behavior according to the reference model for which the input shaper is designed, thus mitigating uncertain system parameters and nonlinear effects. Here, MRAC compares the output of the reference model with the true behavior of the system (nonlinear plant in simulation) and adapts learning parameters while the previously designed input shaper pre-filters steering inputs before being applied to the MRAC loop.

3.1 General Control Scheme

As discussed in section 2.1, the reference model to be used in MRAC is given by Eq. (1), and the plant is a nonlinear system with 18 states. However, the states of interest for the MRAC are simply $\boldsymbol{x} = [\dot{y}\ \ \dot{\psi}]^T$, which in our case proves to be sufficient for the vehicle stability control situation since driving down the error in these 2 states were adequate to achieve desired performance in the control of the plant. Note that this study does not focus on velocity control, and thus, wheel torques in the plant are set to zero. This is a reasonable assumption for high-speed evasive maneuvers where the vehicle's longitudinal velocity could be held nearly constant (e.g., highway emergency lane change whilst in cruise control mode). We realize MRAC as direct adaptive control, i.e. as a feedback controller with gains determined by a nonlinear adaptation scheme that depends only on the chosen output of the system. The extended theory of model-matching conditions is explained in Nguyen (2018), and served as the foundation for the control laws presented in this study.

Equation (1) provides the linear reference model for MRAC, and we refer to the states arising from Eq. (1) driven by the reference input r (here, shaped steering signal) as $\bar{\boldsymbol{x}}$. Our initial assumption for the unknown plant model is of the linear form

$$\dot{\boldsymbol{x}} = A\boldsymbol{x} + \boldsymbol{b}u \tag{4}$$

Now, we assume that we can achieve model matching between the reference model and the unknown plant, i.e., there is an ideal input $\bar{u}$ for Eq. (4) such that the plant states converge to the reference model states $\bar{\boldsymbol{x}}$:

$$\lim_{t\to\infty} \boldsymbol{\varepsilon} = \lim_{t\to\infty} (\bar{\boldsymbol{x}} - \boldsymbol{x}) = \lim_{t\to\infty} \left(\begin{bmatrix} \dot{\bar{y}} \\ \dot{\bar{\psi}} \end{bmatrix} - \begin{bmatrix} \dot{y} \\ \dot{\psi} \end{bmatrix} \right) = \boldsymbol{0}$$

Now, a mapping function between the reference $(\bar{\boldsymbol{x}}, r)$ and ideal-plant trajectories $(\boldsymbol{x}, \bar{u})$ can be expressed as

$$\begin{bmatrix} \boldsymbol{x} \\ \bar{u} \end{bmatrix} = \begin{bmatrix} A_{x\bar{x}} & \boldsymbol{a}_{xr} \\ \boldsymbol{a}_x^T & a_u \end{bmatrix} \begin{bmatrix} \bar{\boldsymbol{x}} \\ r \end{bmatrix} \tag{5}$$

The natural conclusion would be to simply pick $\bar{u}$ from Eq. (5) as a control law for MRAC where $\boldsymbol{a}_x$ and a_u are the true but still unknown control gains, thus yielding the closed-loop dynamics

$$\dot{\boldsymbol{x}} = (A + \boldsymbol{b}\boldsymbol{a}_x^T)\ \boldsymbol{x}\ +\ (\boldsymbol{b}a_u)\ r$$

with $A_r = A + \boldsymbol{b}\boldsymbol{a}_x^T$ and $\boldsymbol{b}_r = \boldsymbol{b}a_u$. However, estimation errors for the control gains must be factored in. We assume these errors to be of the form

$$\begin{bmatrix} \boldsymbol{\Delta a}_x \\ \Delta a_u \end{bmatrix} = \begin{bmatrix} \hat{\boldsymbol{a}}_x - \boldsymbol{a}_x \\ \hat{a}_u - a_u \end{bmatrix} \ . \tag{6}$$

Hence, the closed-loop dynamics of the plant can be rewritten as

$$\dot{\boldsymbol{x}} = (A + \boldsymbol{b}\boldsymbol{a}_x^T + \boldsymbol{b}\boldsymbol{\Delta}\boldsymbol{a}_x^T)\ \boldsymbol{x}\ +\ (\boldsymbol{b}a_u + \boldsymbol{b}\Delta a_u)\ r\ . \tag{7}$$

If the initial assumption in Eq. (4) about the plant being linear does not hold, the above control law does not lead to asymptotic tracking. Hence, the inherent nonlinearities in our true vehicle will cause a state tracking error $\boldsymbol{\varepsilon} \neq \boldsymbol{0}$. For nonlinear plants, a usual assumption in the application of MRAC (Zhang and Wei, 2017) is to lump the nonlinearities together yielding a plant in the form

$$\dot{\boldsymbol{x}} = A\boldsymbol{x} + \boldsymbol{b}u + \boldsymbol{f}(\boldsymbol{x}) \tag{8}$$

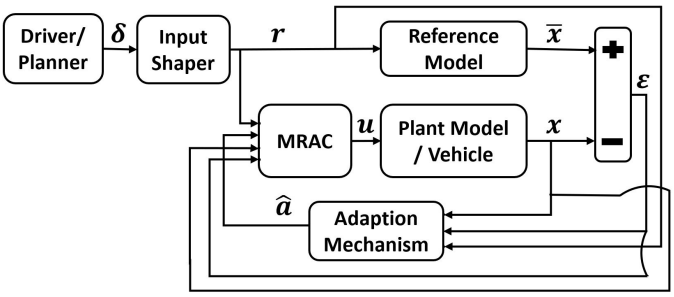

Fig. 4. Block diagram of the MRAC scheme

with the nonlinear portion $\boldsymbol{f}(\boldsymbol{x})$ being linearly parametrizable as $\boldsymbol{f}(\boldsymbol{x}) = \boldsymbol{\Theta}^T\boldsymbol{\Phi}(\boldsymbol{x})$. Here, $\boldsymbol{\Theta}$ is a vector of uncertain parameters that need to be estimated while $\boldsymbol{\Phi}(\boldsymbol{x})$ is a vector of known basis functions. However, the nonlinear plant used in this study cannot be expressed in this manner (this holds for both the simulation model as well as the physical truth for vehicle dynamics). Thus, we introduce a closed-loop feedback term with an online-estimated gain of $\hat{\boldsymbol{a}}_\varepsilon$ to control the error caused by the insufficient input comprised of the feedforward and state feedback terms in Eq. (5). Following a similar approach and adjusting Eqs. (6) and (7) for the additional term leads to closed-loop tracking error dynamics as

$$\dot{\boldsymbol{\varepsilon}} = A_r\boldsymbol{\varepsilon} + \boldsymbol{b}\boldsymbol{\Delta}\boldsymbol{a}_\varepsilon^T\boldsymbol{\varepsilon} - \boldsymbol{b}\boldsymbol{\Delta}\boldsymbol{a}_x^T\boldsymbol{x} - \boldsymbol{b}\Delta a_u r \tag{9}$$

Now, with the 3 gains to be used in the MRAC design finalized, the control law can be defined as

$$u = \hat{\boldsymbol{a}}_x^T\boldsymbol{x} + \hat{a}_u r + \hat{\boldsymbol{a}}_\varepsilon^T\boldsymbol{\varepsilon} \tag{10}$$

Figure 4 now summarizes the control scheme in the graphical form including the inner adaptation loop and the shaping pre-filter.

3.2 Adaption Laws

As just discussed, the adaptation gains $(\hat{\boldsymbol{a}}_x, \hat{\boldsymbol{a}}_\varepsilon, \hat{a}_u,)$ need to be estimated and therefore might not converge to their true values $(\boldsymbol{a}_x, \boldsymbol{a}_\varepsilon, a_u)$. Yet, instability issues can be avoided as long as the adaption/estimation laws for the gains are chosen appropriately. To determine closed loop stability for the proposed control scheme in Eq. (10) in the presence of estimation errors, we employ Lyapunov theory with the following positive definite candidate function:

$$\begin{aligned} V(\boldsymbol{\varepsilon}, \boldsymbol{\Delta a}_x, \Delta a_u, \boldsymbol{\Delta a}_\varepsilon) = \\ \boldsymbol{\varepsilon}^T P\boldsymbol{\varepsilon} + \mathrm{tr}(\boldsymbol{\Delta a}_x^T\Gamma_x^{-1}\boldsymbol{\Delta a}_x) + (\Delta a_u\Gamma_u^{-1}\Delta a_u) \\ + \mathrm{tr}(\boldsymbol{\Delta a}_\varepsilon^T\Gamma_\varepsilon^{-1}\boldsymbol{\Delta a}_\varepsilon)\ . \end{aligned} \tag{11}$$

Here, Γ and P are symmetric positive definite matrices. While Γ can be any such matrix, P is a unique solution to the algebraic Lyapunov equation

$$PA_r + A_r^T P = -Q \tag{12}$$

with Q being any symmetric positive definite matrix.

Equation (11) can be abbreviated as $V = V_1 + V_2$. For stability, the time-derivative of the Lyapunov function is required to be negative semi-definite. In order to show this property, $\dot{V}_1$ can be evaluated as

$$\begin{aligned} \dot{V}_1 &= \boldsymbol{\varepsilon}^T P\dot{\boldsymbol{\varepsilon}} + \dot{\boldsymbol{\varepsilon}}^T P\boldsymbol{\varepsilon} \\ &= -\boldsymbol{\varepsilon}^T Q\boldsymbol{\varepsilon} + 2\boldsymbol{\varepsilon}^T P[\boldsymbol{b}\boldsymbol{\Delta}\boldsymbol{a}_\varepsilon^T\boldsymbol{\varepsilon} - \boldsymbol{b}\boldsymbol{\Delta}\boldsymbol{a}_x^T\boldsymbol{x} - \boldsymbol{b}\Delta a_u r]\ . \end{aligned}$$

where Eqs. (9) and Eq. (12) have been employed. Now, we can utilize the trace property $\mathrm{tr}(MN^T) = N^T M$ on the terms in $\dot{V}_1$, i.e.

$$\boldsymbol{\varepsilon}^T P \boldsymbol{b} \boldsymbol{\Delta a}^T \boldsymbol{\Omega} = \mathrm{tr}(\boldsymbol{\Delta a}^T \boldsymbol{\Omega} \boldsymbol{\varepsilon}^T P \boldsymbol{b})$$

where $\boldsymbol{\Delta a}$ was used as a placeholder for $\boldsymbol{\Delta a}_x/\Delta a_u/\boldsymbol{\Delta a}_\varepsilon$ and $\boldsymbol{\Omega}$ for $\boldsymbol{x}/r/\boldsymbol{\varepsilon}$. Similarly, $\dot{V}_2$ can be simplified by using $\boldsymbol{\Delta a}$ as above, yielding

$$\begin{aligned}\dot{V}_2 &= \mathrm{tr}(\boldsymbol{\Delta \dot{a}}^T \Gamma^{-1} \boldsymbol{\Delta a} + \boldsymbol{\Delta a}^T \Gamma^{-1} \boldsymbol{\Delta \dot{a}}) \\ &= 2\,\mathrm{tr}(\boldsymbol{\Delta \dot{a}} \Gamma^{-1} \boldsymbol{\Delta a}^T)\end{aligned}$$

where Γ has been used as an encompassing term for $\Gamma_x/\Gamma_u/\Gamma_\varepsilon$. Thus, combining $\dot{V}_1$ and $\dot{V}_2$ then results as

$$\begin{aligned}\dot{V} = &-\boldsymbol{\varepsilon}^T Q \boldsymbol{\varepsilon} + 2\,\mathrm{tr}(\boldsymbol{\Delta a}_x[-\boldsymbol{x}\boldsymbol{\varepsilon}^T P \boldsymbol{b} + \Gamma_x^{-1} \boldsymbol{\Delta \dot{a}}_x^T]) \\ &+ 2\,\mathrm{tr}(\Delta a_u[-r\boldsymbol{\varepsilon}^T P \boldsymbol{b} + \Gamma_u^{-1} \Delta \dot{a}_u^T]) \\ &+ 2\,\mathrm{tr}(\boldsymbol{\Delta a}_\varepsilon[\boldsymbol{\varepsilon}\boldsymbol{\varepsilon}^T P \boldsymbol{b} + \Gamma_\varepsilon^{-1} \boldsymbol{\Delta \dot{a}}_\varepsilon^T]) \qquad (13)\end{aligned}$$

In order to ensure $\dot{V}$ to be negative semi-definite, the gains now can be chosen in adaptive fashion as

$$\begin{aligned}\dot{\hat{\boldsymbol{a}}}_x &= \Gamma_x \boldsymbol{x} \boldsymbol{\varepsilon}^T P \boldsymbol{b} \\ \dot{\hat{a}}_u &= \Gamma_u r \boldsymbol{\varepsilon}^T P \boldsymbol{b} \\ \dot{\hat{\boldsymbol{a}}}_\varepsilon &= -\Gamma_\varepsilon \boldsymbol{\varepsilon}\boldsymbol{\varepsilon}^T P \boldsymbol{b}\,. \qquad (14)\end{aligned}$$

These result in the negative semi-definite quadratic form $\dot{V} = -\boldsymbol{\varepsilon}^T Q \boldsymbol{\varepsilon} \leq \mathbf{0}$ (substituting Eq. (14) in Eq. (13)), thus proving Lyapunov stability. Additionally, $\dot{V}$ satisfies $\lim_{t\to\infty} ||\boldsymbol{\varepsilon}|| = 0$ which indicates asymptotic tracking and boundedness.

The Γ matrices are called learning rates and determine the speed at which the errors settle to their minimum value (ideally 0). The success of this control design will depend on the learning and adaptation speed of the MRAC loop in comparison to the vehicle's eigenvalues and maneuver length. While $\boldsymbol{b}$ is treated as an unknown in Eq. (8), the adaptation laws in Eq. (14) assume knowledge of the control gain matrix. In many applications - including our plant - $\boldsymbol{b}$ is not fully known, and the control input is included in the general form $\dot{\mathbf{x}} = \boldsymbol{f}(\mathbf{x}, u)$. In the current approach, we adjust for differences between $\boldsymbol{b}_r$ and $\boldsymbol{b}$ by the simple introduction of a manually pre-tuned correction factor $\lambda > 0$, i.e., $\boldsymbol{b} = \boldsymbol{b}_r \lambda$.

4. NUMERICAL RESULTS

To validate our control performance, we have chosen 2 maneuvers: (i) double lane change; and (ii) sine wave. These are aggressive maneuvers at the selected speeds of 80 and 120 km/h exciting nonlinear behavior and parameter changes. The vehicle response plots are shown in Fig. 5. Here, we do not include the response of an uncontrolled/open loop vehicle, as the superior performance of the stand-alone input shaper has already been shown in Fig. 3.

As evident, the MRAC enforces linearity in the vehicle throughout the maneuver despite the rapid change of parameters (e.g., cornering stiffness). It can also be seen from the response to the sinusoidal reference that the control input settles quickly despite some initial oscillations. For boundedness and convergence analysis as indicated in section 3, the DLC maneuver at 120 km/h is most suited. At this speed and at this repetition rate, the uncontrolled

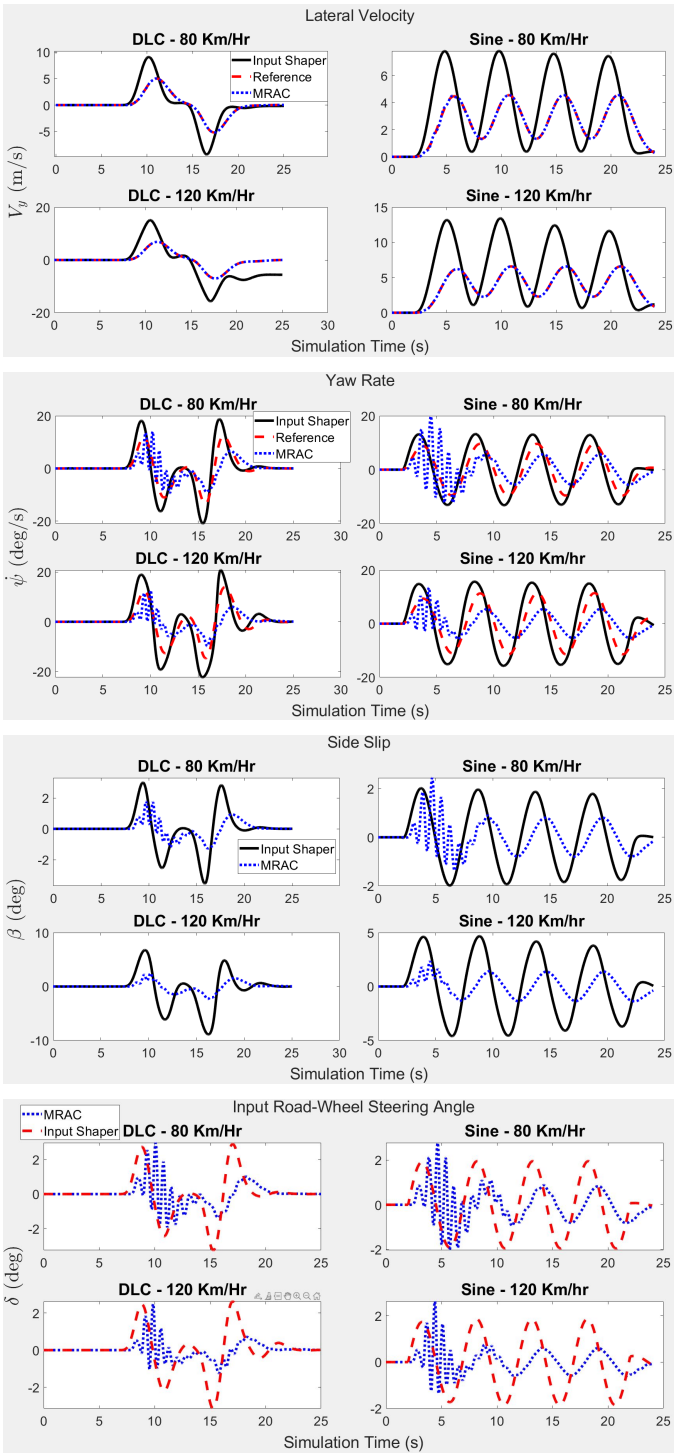

Fig. 5. Vehicle responses for double lane change and sinusoidal maneuver

vehicle's behavior deviates largely and rapidly from the reference behavior as nonlinear effects accumulate. Figure 6 shows the vehicle's states under persistent DLC maneuvers and illustrates how well the MRAC-input shaper framework tracks the reference states. The convergence of the adaptation gains is also demonstrated in Fig. 7. The underlying code generating a variety of additional plots can be found in Srinivasan (2021). Here, the boundedness of the inputs can also be inferred from simulations.

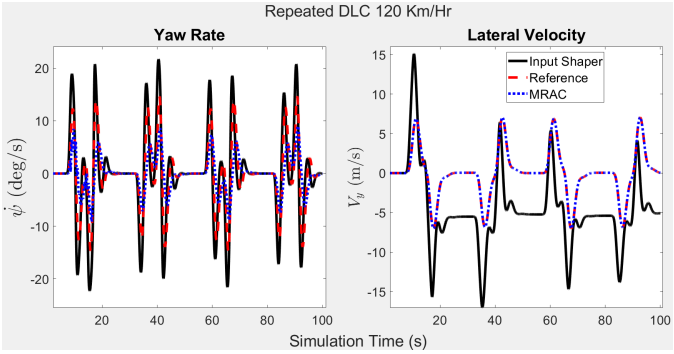

Fig. 6. Yaw rate and lateral velocity under persistent DLC inputs

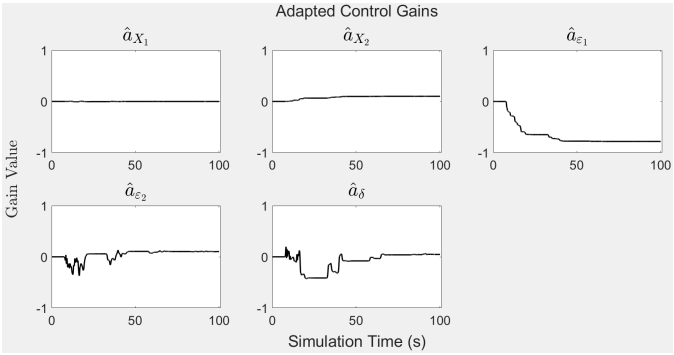

Fig. 7. Adaptation gains convergence

5. DISCUSSION AND FUTURE WORK

In this study, we explored an adaptive control framework to enable a steer-by-wire vehicle operating in the nonlinear range while tracking a reference trajectory. A direct adaptive controller was developed to significantly advance our previous work in reference shaping control for road vehicles. Boundedness, stability, and asymptotic tracking for the MRAC framework were demonstrated via a theoretical approach as well as numerically. For the numerical studies, the success of the new control framework was shown for a high fidelity vehicle model subject to aggressive maneuvers at high velocities. Errors and gains converged to a steady-state as indicated by the Lyapunov analysis. For our future work, we plan to further expand the adaptive control approach in presence of other factors, such as measurement noise, changing surface conditions, etc. An analysis of the real-time performance of the suggested controller using a Hardware-in-Loop (HiL) approach is also part of our future scope.

REFERENCES

Ahmadian, N., Khosravi, A., and Sarhadi, P. (2021). Driver assistant yaw stability control via integration of afs and dyc. *Vehicle System Dynamics*, 1–21.

Arango, J.F., Bergasa, L.M., Revenga, P.A., Barea, R., López-Guillén, E., Gómez-Huélamo, C., Araluce, J., and Gutiérrez, R. (2020). Drive-by-wire development process based on ros for an autonomous electric vehicle. *Sensors*, 20(21), 6121.

Byrne, R. and Abdallah, C. (1995). Design of a model reference adaptive controller for vehicle road following. *Mathematical and Computer Modelling*, 22(4-7), 343–354.

Campbell, M., Egerstedt, M., How, J.P., and Murray, R.M. (2010). Autonomous driving in urban environments: approaches, lessons and challenges. *Philosophical Transactions of the Royal Society A: Mathematical, Physical and Engineering Sciences*, 368(1928), 4649–4672.

Fancher, P., Segel, L., Bernard, J., and Ervin, R. (1976). Test procedures for studying vehicle dynamics in lane-change maneuvers. *SAE Technical Paper Series*.

Fukao, T., Miyasaka, S., Mori, K., Adachi, N., and Osuka, K. (2001). Active steering systems based on model reference adaptive nonlinear control. *IEEE Intelligent Transportation Systems (ITSC). Proceedings*.

Kalra, N. (2017). *Challenges and Approaches to Realizing Autonomous Vehicle Safety*. RAND Corporation.

Kalur, A., Shivakumar, K., Schmid, M., and Crassidis, J.L. (2016). Adaptive control for spacecraft formation flying with solar radiation pressure and reduction of secular drift. *American Control Conference (ACC)*.

Khorrami, F., Jain, S., and Tzes, A. (1993). Adaptive nonlinear control and input preshaping for flexible-link manipulators. *1993 American Control Conference*.

Mitov, A., Kralev, J., Slavov, T., and Angelov, I. (2020). Model reference adaptive control for steering application of agriculture machines. *7th International Conference on Energy Efficiency and Agricultural Engineering*.

Nguyen, N.T. (2018). *Model-reference adaptive control*. Springer International Publishing.

Pacejka, H.B. (2009). *Tyre and vehicle dynamics*. Elsevier Butterworth-Heinemann.

Rajamani, R. (2012). *Vehicle dynamics and control*. Springer.

Singh, T. (2019). *Optimal reference shaping for dynamical systems: Theory and applications*. CRC Press.

Slotine, J.J.E. and Li, W. (2005). *Applied nonlinear control*. Pearson Education Taiwan.

Srinivasan, S. (2021). Code for adaptive and reference shaping control for steer-by-wire vehicles in high speed maneuvers. `https://github.com/srivats2794/Adaptive_Control_SteerByWire`.

Srinivasan, S., Schmid, M.J., and Krovi, V.N. (2019). Analysis of reference shaping control for improved yaw stability in a steer-by-wire vehicle. *Volume 3, Rapid Fire Interactive Presentations: Automotive and Transportation Systems*.

Tzes, A. and Yurkovich, S. (1993). An adaptive input shaping control scheme for vibration suppression in slewing flexible structures. *IEEE Transactions on Control Systems Technology*, 1(2), 114–121.

Vempaty, S., Lee, E., and He, Y. (2016). Model-reference based adaptive control for enhancing lateral stability of car-trailer systems. *Volume 12: Transportation Systems*.

Yamaguchi, Y. and Murakami, T. (2009). Adaptive control for virtual steering characteristics on electric vehicle using steer-by-wire system. *IEEE Transactions on Industrial Electronics*, 56(5), 1585–1594.

Yih, P. and Gerdes, J. (2005). Modification of vehicle handling characteristics via steer-by-wire. *IEEE Transactions on Control Systems Technology*, 13(6), 965–976.

Zhang, D. and Wei, B. (2017). A review on model reference adaptive control of robotic manipulators. *Annual Reviews in Control*, 43, 188–198.